Optical study of spin-flip transitions at Fe^{3+} in InP

K. Pressel, G. Bohnert, A. Dörnen, and B. Kaufmann

IV. Physikalisches Institut, Universität Stuttgart, D-7000 Stuttgart 80, Germany

J. Denzel and K. Thonke

Abteilung Halbleiterphysik, Universität Ulm, D-7900 Ulm, Germany

(Received 30 April 1992)

The 0.5-eV (4000-cm^{-1}) emission band in InP:Fe is studied in detail by Fourier-transform infrared photoluminescence (PL), time-resolved PL, and photoluminescence excitation (PLE) spectroscopy. We resolve new fine structures in both the zero-phonon (ZP) lines and in the corresponding phonon sideband. The transient PL signal follows an exponential decay with a time constant of 1.1 ± 0.3 ms. The PLE shows that the 0.5-eV band can be pumped via hole capture of Fe^{2+} and even more efficiently by exciting resonantly the charge-transfer states $[Fe^{2+}(^5T_2), h_b]$, where the hole is bound to Fe^{2+}. The results from PLE and the long decay time strongly support the interpretation of the 0.5-eV band as spin-flip transitions $^4T_1 \rightarrow {}^6A_1$ of Fe^{3+}. We explain the fine structure of the ZP lines by a dynamic Jahn-Teller distortion in the excited state $^4T_1$. The decay of the charge-transfer states $[Fe^{2+}(^5T_2), h_b]$ leaves the Fe^{3+} ion in an excited state $(Fe^{3+})^*$, which pumps the 0.5-eV emission.

I. INTRODUCTION

Indium phosphide doped with iron shows a semi-insulating character with resistivities of up to 10^8 Ω cm.[1] Semi-insulating InP is desirable as substrate material for optoelectronic devices such as $In_xGa_{1-x}As$ lasers, light emitting diodes, etc. But as Fe acts as an efficient recombination center it also limits the device performance. Thus it is important to understand the interaction of the deep acceptor trap Fe with free carriers.

In InP the existence of Fe in the charge state 3+ ($3d^5$, $L = 0$, $S = \frac{5}{2}$) has been shown by electron paramagnetic resonance (Koschel, Kaufmann, and Bishop).[2] The existence of Fe in the charge state 2+ ($3d^6$, $L = 2$, $S = 2$) was revealed in optical measurements.[2] Both the Fe^{3+} and the Fe^{2+} ions are located on the In site in a tetrahedral environment of phosphorus. The ^5D ground state of the Fe^{2+} ion splits in the tetrahedral crystal field into a $^5T_2$ excited state and ^5E ground state. These states are further split by spin-orbit coupling into six and five levels, respectively. The characteristic four-line spectrum at ≈ 2800 cm^{-1} (0.35 eV) observed by photoluminescence (PL) and optical-absorption spectroscopy is a finger print of Fe^{2+}. Recently, Pressel *et al.*[3] and Thonke and Pressel[4] have investigated these transitions with an improved signal-to-noise ratio by optical Fourier-transform-infrared (FTIR) spectroscopy. They give a complete level scheme for Fe^{2+} including the series of excited states of the $^5T_2$ level.

An additional Fe-related emission is observed in InP:Fe at about 4000 cm^{-1} (0.5 eV). This emission has been studied only in three publications and is discussed controversially up to now. Tapster *et al.*[5] and Leyral *et al.*[6] show the rough features of the 4000-cm^{-1} emission. The spectra revealed a weak zero-phonon (ZP) line at 4300

cm^{-1} and a characteristic relatively strong phonon sideband. Photoluminescence excitation (PLE) experiments performed with the light of a tungsten-halogen lamp and dispersed by a monochromator show a broad band with an onset at $h\nu > 1.2$ eV.[6] Both groups give no clear assignment and independently speculate that either Fe-related complexes or charge-transfer (CT) transitions of the type $[Fe^{2+}(^5T_2), h_b] \rightarrow Fe^{3+} + h\nu(0.5$ eV$)$ might be responsible for the 0.5-eV band. Leyral *et al.*[6] also mentioned the possibility that a transition metal other than Fe might be involved. The third contribution was published by Deveaud *et al.*[7] in 1984. They performed temperature-dependent PL studies on the 0.5-eV band and observed a hot line at 4323 cm^{-1}. They attributed the emission to an internal $3d$ spin-flip transition ($\Delta S = 1$): $^4T_1 \rightarrow {}^6A_1$ of Fe^{3+}. The assignment was derived from the long decay time of 1.5 ms found for the PL signal by the above band-gap excitation. In that paper the PL transient was not shown and no comparison with the decay time of the Fe^{2+} luminescence of the same sample was made.

In this paper we present a detailed study of the 0.5-eV emission by high sensitive optical FTIR PL and absorption spectroscopy, time-resolved PL studies, and photoluminescence excitation spectroscopy (PLE). Our data confirm the assignment of the 0.5-eV luminescence to Fe^{3+} as concluded by Deveaud *et al.*[7] Additionally, we introduce a model for the excitation mechanism of this emission.

II. EXPERIMENTAL DETAILS

In the PL experiments the samples were excited either by a Kr-ion laser (647 nm) or by a Ti/sapphire laser

which is tunable between 1.1- and 0.85-μm wavelength. The latter excitation source was used when band-band excitation of the host material was not intended. The emission light was analyzed by a BOMEM DA3.01 FTIR spectrometer that offers a minimum unapodized resolution of 0.01 cm^{-1}. All the PL spectra were detected by a liquid-nitrogen-cooled InSb detector. The FTIR absorption spectra in the energy range at about 1.13 eV were recorded by an In$_x$Ga$_{1-x}$As diode.

In the PLE studies, where either the 2800-cm^{-1} (0.35-eV) emission of Fe^{2+} or the 4000-cm^{-1} (0.5-eV) band were monitored, the samples were excited by the tunable Ti/sapphire laser. The PLE measurements were performed by a conventional optical setup using a 3/4m Spex monochromator and a PbS detector (190 K) in the monitor path.

For time-resolved studies the samples were excited by the 1.06-μm line of a pulsed Nd:YAG (yttrium aluminum garnet) laser in Q-switch operation. The luminescence light was dispersed by a 3/4m Spex monochromator and detection was performed by an InSb detector which was connected to a real-time transient averager. The time resolution of the whole setup was $\approx$ 100 ns. The samples were grown by the liquid-encapsulated Czochralski method and were semi-insulating or showed n-type conductivity.

III. RESULTS

A. cw photoluminescence: Zero-phonon lines and phonon replicas

In accordance with Tapster *et al.*[5] we only observed the 0.5-eV emission in Fe-doped samples which showed the characteristic four Fe^{2+} emission lines, too. Figure 1 shows a typical FTIR emission spectrum of the 0.5-eV band at 2 K between 3500 and 4400 cm^{-1}. The excitation wavelength of the Ti/sapphire laser was set to 1 μm. Thus luminescence was not excited via band-band excitation. The luminescence intensity obtained with an excitation wavelength of 647 nm is comparable. Hence the 0.5-eV band can be pumped efficiently without band-band excitation, as reported by Leyral *et al.*[6] Due to the

improved sensitivity of FTIR PL spectroscopy the spectrum in Fig. 1 shows much more details than the spectra published hitherto.[5-7] Different to Ref. 7 we resolve at low temperature two ZP lines at 4301.19 cm^{-1} (ZP1) and 4305.33 cm^{-1} (ZP2), which appear to have half-widths of less than 0.3 cm^{-1}. The two ZP lines are shown in more detail in the right inset of Fig. 1.

Figure 2 shows three emission spectra in the range between 3930 and 4400 cm^{-1} which were detected at different sample temperatures. We clearly observe that the intensity ratio ZP2/ZP1 increases with rising temperature. Already at 4.2 K the intensity ratio changes to > 1. In the 12-K spectrum a second hot line at 4323 cm^{-1} (ZP3) shows up which was already observed by Deveaud *et al.*[7] Because of the larger half-width of ZP3 at 12 K compared to ZP2 we cannot decide whether it consists of two lines or not. Hence the initial state of the emission must at least be split threefold. The upper states are separated by 4.14 and 22 cm^{-1} from the lowest excited state, respectively.

The ZP lines show a strong and structured phonon sideband, which consists on the one hand of broad bands due to coupling to lattice phonons and on the other hand of sharp lines due to coupling to defect-specific vibrational gap modes and vibrational resonant modes. The sideband is depicted in Figs. 1 and 2. Couplings of the ZP transitions to a specific vibrational mode are indicated by a rake. The replicas of the defect-specific vibrational modes are listed in Table I.

At 4240 cm^{-1} a broad asymmetric emission is observed (Fig. 2). Because of the spacing of the maximum of 65 cm^{-1} from the ZP lines we attribute this hump to a superposition of TA(X) ($h\nu_{TA(X)}$ = 67 cm^{-1}) and TA(L) ($h\nu_{TA(L)}$ = 54 cm^{-1}) phonons that couple to the ZP transitions. The positions of the TA(X) and TA(L) phonons according to Ref. 8 are indicated by arrows. Between 3980 and 3995 cm^{-1} coupling to TO lattice phonons is resolved (Fig. 1, left inset). The strongest coupling to lattice phonons occurs for LO-type modes, which show up between 3950 and 3965 cm^{-1} (Fig. 1, left inset).

In the range between 3960 and 4020 cm^{-1} we observe the coupling of the ZP lines to a series of very sharp phonons (Fig. 1, left inset). Due to the small half-widths
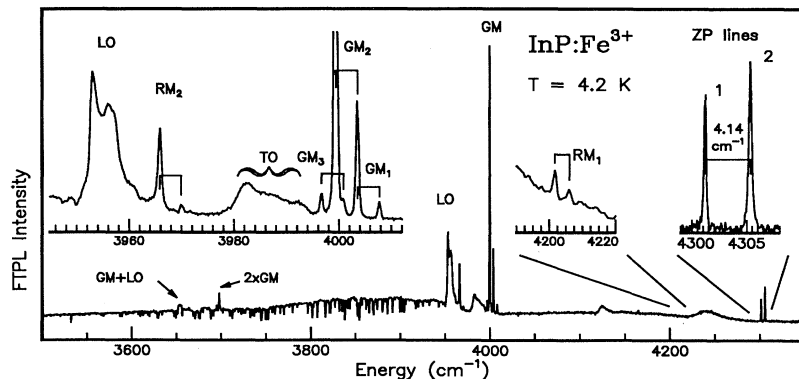

FIG. 1. Photoluminescence spectrum of the 0.5-eV emission of SI-InP:Fe which is attributed to the $^4T_1 \rightarrow {}^6A_1$ intra 3d transitions of Fe^{3+}. Beside the two ZP lines ZP1 and ZP2 we observe a characteristic phonon sideband, where sharp Fe defect-specific phonons GM$_1$-GM$_3$ and their multiples are superimposed. This spectrum was recorded at 4.2-K sample temperature with a resolution of 0.5 cm^{-1}. The part of the spectrum between 3600 and 4000 cm^{-1} is obscured by absorptions due to water vapor. The right inset shows with higher resolution (0.2 cm^{-1}) the two ZP lines, which have a spacing of 4.14 cm^{-1}. In the two other insets the phonon replicas around 4000 and 4200 cm^{-1} are shown in an expanded scale (resolution = 0.5 cm^{-1}).
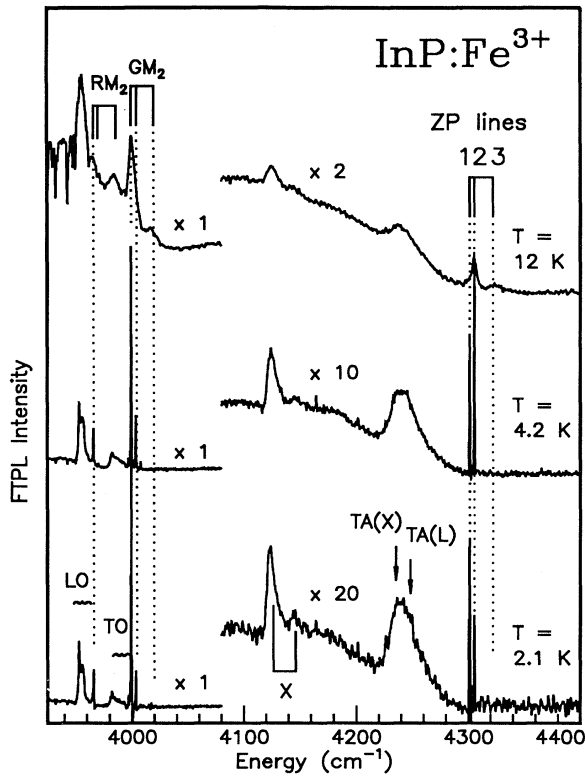
FIG. 2. Temperature dependence of the 0.5-eV emission of SI-InP:Fe. The spectra reveal that ZP2 is a hot line. Additionally a second hot line at 4323 cm^{-1} shows up in the 12-K spectrum. Furthermore, we observe the temperature dependence of the various phonons [TA(X), TA(L), TO, and LO] couplings and the temperature-dependence of the Fe defect-specific modes GM$_2$ (301.7 cm^{-1}) and RM$_2$ (335.4 cm^{-1}). The structure X might be due to transitions from a highly excited state $(Fe^{3+})^*$, e.g., ^4F or ^4P to the first excited state of $^4T_1(^4G)$ of Fe^{3+} (see also Figs. 5 and 6).

and optical lattice phonons we denote them as "resonant mode" RM$_1$ and RM$_2$, respectively. At 4.2 K a trace of coupling to ZP2 is observed for both modes.

At 4124 and 4146 cm^{-1} we find a feature labeled "X" (Fig. 2). For two reasons this emission cannot simply be assigned to coupling to a single lattice phonon. (i) The spacing of about 180 cm^{-1} to the ZP lines is in the gap of the phonon-dispersion curve. Energetically it could be a combination mode by coupling to a LA(X) ($h\nu_{LA(X)}$ = 120 cm^{-1}) and a TA phonon. But it is difficult to understand why coupling to the LA(X) phonon is not observed. We also exclude coupling of the ZP lines to a defect-specific mode, because in such a case we would expect sharp lines. (ii) A second more important reason is that the lines of X do not thermalize, as found for the other phonon replica mentioned above. A possible explanation for the feature X will be given in Sec. IV.

B. Time-resolved studies and PL excitation spectroscopy

To distinguish whether or not the 0.5-eV band is correlated with the Fe^{2+} luminescence at $\approx$ 2800 cm^{-1} (0.35 eV) we performed time-resolved measurements by using the 1.06-μm line of a Nd:YAG laser for below-band-gap excitation. Figure 3 shows the decay of the 0.5-eV emission which is exponential within experimental uncertainty. From the transient a decay time of 1.1 ± 0.3 ms can be determined. This value agrees quite well with the 1.5 ms obtained by Deveaud et al.[7] who used above-band-gap excitation. The inset in Fig. 3 shows the exponential decay of the Fe^{2+} (0.35-eV) emission measured on the same sample. In accordance with Klein, Furneaux, and Henry,[9] who used above-band-gap excitation, we find a decay time of 10 μs at 8 K.

We now consider the excitation mechanism of Fe^{2+} and

(HW) of less than 0.5 cm^{-1} we partly attribute the lines to Fe-defect-specific modes. The most intense line at 3999.4 cm^{-1} has a distance of 301.7 cm^{-1} from ZP1. This value is close to the energy of the LO phonon.[8] Nonetheless we attribute this line to a defect-specific gap mode (GM$_2$), because of the rather small half-width of 0.32 cm^{-1}. A coupling of GM$_2$ to ZP2 shows up 4.14 cm^{-1} higher in energy. We note that the coupling of GM$_2$ to ZP1 is five times larger as compared to the coupling of ZP2. The "hot line" at 4023 cm^{-1} obviously belongs to coupling of ZP3 to GM$_2$ (Fig. 2). Much weaker couplings to gap modes GM$_1$ and GM$_3$ are assigned as given in Fig. 1 and listed in Table I. In Sec. IV we will discuss why the GM$_2$ replica is much stronger than the ZP transitions. At about 3700 cm^{-1} (see Fig. 1) coupling to 2×GM$_2$ and combinations of GM$_2$ with LO-phonon replicas are observed.

At 3965.9 (3970.0 cm^{-1}) and 4201.8 cm^{-1} (4206.0 cm^{-1}) we observe coupling of ZP1 (ZP2) to further defect-specific vibrational modes (Figs. 1 and 2). Since these modes are energetically degenerate with acoustical
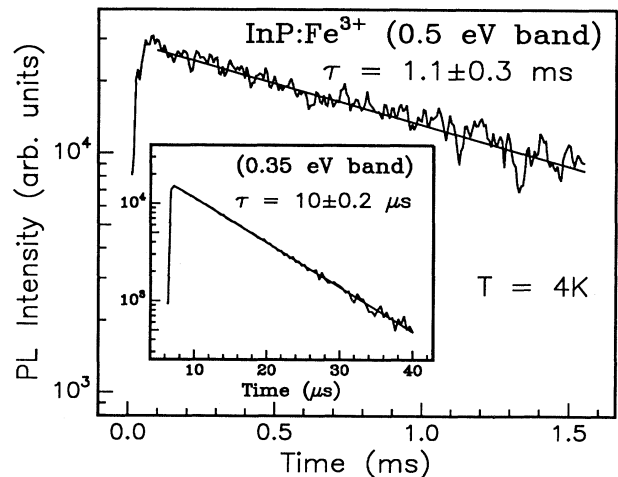

FIG. 3. Decay of the 0.5-eV (Fe^{3+}) and 0.35-eV (Fe^{2+}, inset) PL emissions in InP measured on the same sample. The decay time of the 0.5-eV luminescence is 1.1 ms, whereas a time constant of 10 μs is found for the 0.35-eV luminescence.

TABLE I. Spectral values for the ZP lines and some phonon replicas taken from a spectrum recorded at 4.2-K sample temperature with a resolution of 0.2 cm^{-1}. The accuracy of the energy position is ≤ 0.1 cm^{-1}. Amplitudes are normalized to line ZP1. All lines exhibit Lorentzian shape. The half-width is given as full width at half maximum (FWHM).

| Energy | Amplitude | FWHM | Spacing from | | Interpretation |
| | | | ZP1 | ZP2 | |
(cm^{-1})		(cm^{-1})	(cm^{-1})	(cm^{-1})	
4301.19	1	0.26			ZP1
4305.33	1.4	0.26	4.14		ZP2
4323	<1	2	22		ZP3
3965.9	1.68	0.52	−335.3		RM$_2$
3970.0	0.23	0.52		−335.3	RM$_2$
3996.7	0.85	0.32	−304.5		GM$_3$
3999.4	16.6	0.32	−301.7		GM$_2$
4000.9	0.28	0.32		−304.4	GM$_3$
4003.6	3.98	0.32	−297.6	−301.7	GM$_1$, GM$_2$
4007.8	0.57	0.32		−297.5	GM$_1$
4201.8	<1	<1	−99.4		RM$_1$
4206.0	<1	<1		−99.3	RM$_1$

the 0.5-eV band. Figure 4 compares three different optical spectra of the region close to the hole-photoionization threshold [Fe^{3+} + $h\nu$ → Fe^{2+}($^5T_2$) + h] at 9100 cm^{-1} (1.13 eV): (i) an absorption spectrum [Fig. 4(a)], (ii) a PLE spectrum using the 0.5-eV band luminescence as a monitor [Fig. 4(b)], (iii) a PLE spectrum using the Fe^{2+} luminescence (0.35 eV) as a monitor [Fig. 4(c)].

The transitions shown in Fig. 4(a) were recently assigned by Thonke and Pressel[4] to charge-transfer (CT) transitions: Fe^{3+} + $h\nu$ → [Fe^{2+}($^5T_2$), h_b]. In the charge-transfer state [Fe^{2+}, h_b] the hole is not completely ionized, but bound in effective-mass-like states by the Coulomb attraction of the negatively charged Fe^{2+} ion. Thus this absorption spectrum reflects both the excited states of the $^5T_2$ manifold of Fe^{2+} (J=1, 2, and 3) and the effective-mass (EM) series of h_b. The labeling of the lines is according to Ref. 4. A, B, and C denote the states of $^5T_2$. The fine structure of each series, which arises from the EM states of the bound hole, is marked by the lower indices, e.g., $A_1, \ldots, A_3$. Please note that in Fig. 4 the vibrational modes LM1* and GM1* and the corresponding phonon energies refer to Fe^{2+},[3] not to the 0.5-eV band.

Figure 4(b) shows a detailed PL excitation spectrum of the 0.5-eV band. For the best signal-to-noise ratio we chose as the monitor the GM$_2$ phonon replica at 4000 cm^{-1}, the most intense line in the 0.5-eV emission band. The fine structures of the excitation spectrum are identical to those in the absorption spectrum of InP:Fe. Obviously, there exists an efficient energy transfer from the bound CT states [Fe^{2+}($^5T_2$), h_b] to the excited states of the 0.5-eV center.

Figure 4(c) shows an excitation spectrum of the Fe^{2+} emission. The monitor energy was set to 2830 cm^{-1}, which is the energy of the strongest PL line of the Fe^{2+} transitions. The pronounced onset at 9100 cm^{-1} is due
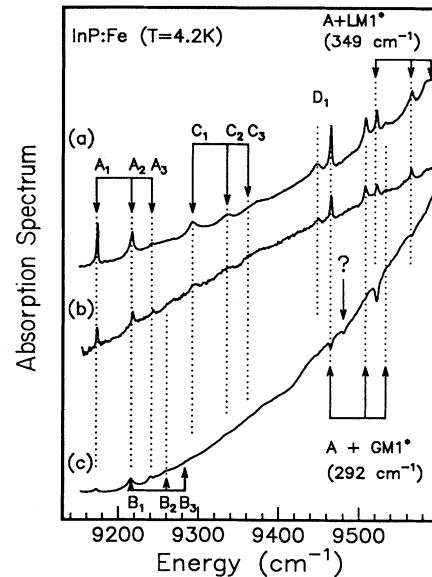

FIG. 4. (a) Absorption spectrum of SI-InP:Fe at the photoionization threshold of 1.13 eV (9100 cm^{-1}). The fine structure belongs to charge-transfer transitions of the type Fe^{3+} + $h\nu$ → [Fe^{2+}($^5T_2$), h_b]. The A series belongs to a two-particle final state where the Fe^{2+} ion is excited in the ground state of the $^5T_2$ manifold and the hole is in various excited states. (b) PLE spectrum of Fe^{3+}(0.5-eV emission) in InP. The spectrum shows the same fine-structure lines as the absorption spectrum above. (c) PLE spectrum of Fe^{2+}-related internal 3d emissions. While the A series appears as positive features in the phonon sideband several phonon replica show up as dips. The dip which is marked by "?" does not fit to any Fe-related resonances found in (a) or (b). The nature of this feature remains unknown up to now. (Note, the vibrational modes LM1* and GM1* and the corresponding phonon energies refer to Fe^{2+}, see Ref. 3.)

to the photoionization [$Fe^{3+} + h\nu \rightarrow Fe^{2+}(^5T_2) + h$] as observed by Leyral et al.[6] Since we use a Ti/sapphire laser for excitation in our measurements the resolution is much higher than in Ref. 6. Therefore additional sharp structures superimposed on the photoionization band show up. We observe the fine structure lines A_1 to A_3 as minor peaks, whereas the resonances of A_1+GM1* and A_1+LM1* appear as dips, respectively. The transitions C_1 to C_3 are hardly resolvable. The comparison of Figs. 4(a), 4(b), and 4(c) shows that the absorption spectrum is closer connected to the PLE spectrum of the 0.5-eV band than to the PLE spectrum of the 0.35-eV band.

In Ref. 4 it was pointed out that a series B_1 through B_3 should exist, where the line B_1 energetically overlaps with A_2. Both in the excitation spectrum of Fe^{3+} [Fig. 4(b)] and in the excitation spectrum of Fe^{2+} [Fig. 4(c)] we observe a peak at the expected position of B_2. The spacing between the peaks B_2 and $B_1(A_2)$ perfectly agrees with the spacing of A_2 and A_1. Thus from PLE we get evidence for the three CT transitions B_1 to B_3 as indicated by the rake in Fig. 4.

IV. DISCUSSION

Tapster et al.[5] and Leyral et al.[6] suggested that the 0.5-eV band could be due to a CT transition: [$Fe^{2+}(^5T_2)$, h_b] $\rightarrow$ $Fe^{3+} + h\nu(0.5$ eV). As mentioned in Sec. III these CT transitions have recently been identified.[4] Thus the explanation of the 0.5-eV luminescence as a CT transition must be excluded.

It has also been suggested from time-resolved PL (Ref. 7) that the 0.5-eV luminescence is related to the spin-flip transition between a $^4T_1$ excited state and a $^6A_1$ ground state of $Fe^{3+}(3d^5)$. The data reported here, namely, the fine structure observed in the ZP lines, the decay time of the PL signal, and the PLE spectra, are fully in accordance with this interpretation. In the following we will discuss the results in this respect. We discard the explanations that involve Fe-related complexes or other transition-metal impurities.

Figure 5 shows the crystal-field states of a $3d^5$ electron configuration in a tetrahedral environment as it applies to the Fe^{3+} ion in InP.[10] The $^6A_1$ ground state of Fe^{3+} ($3d^5$, $L = 0$, $S = \frac{5}{2}$) is split into two states (Γ_8 and Γ_7) which are separated by 0.07 cm^{-1}.[2] This splitting is obscured by the half-width of the transitions. The ^4G first excited state splits by the T_d crystal field into four sublevels, where the lowest state is a $^4T_1$ level. In Fig. 5 also the higher excited states of the Fe^{3+} ion in a tetrahedral crystal field are depicted schematically (compare, e.g., the results for Mn^{2+} in ZnS, which is isoelectronic to Fe^{3+}, Ref. 10). Additional spin-orbit coupling splits the $^4T_1$ state further into four sublevels Γ_6, Γ_8, Γ_7, and Γ_8. According to crystal-field theory the states are separated by ≈ 100 cm^{-1}. As shown by Koidl[11] a dynamic Jahn-Teller effect can drastically reduce the pure crystal-field splitting of the $^4T_1$ states by coupling to an ε-type phonon. In the static limit the four sublevels coincide in pairs [(Γ_8, Γ_7) and (Γ_6, Γ_8)]. Several $3d^5$ systems, which show this behavior, have been reported in the literature.
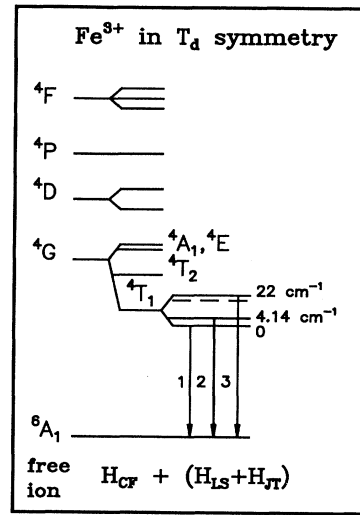

FIG. 5. Level scheme of the Fe^{3+} ion in a tetrahedral crystal field. The $^6A_1$ ground state is split into a Γ_8 and a Γ_7 state not resolved here. The ^4G first excited state is split into four sublevels in a tetrahedral environment. The $^4T_1$ ground state is further split by spin-orbit coupling into four levels, which can be significantly influenced by a dynamic Jahn-Teller distortion. On the right side the spacing of the $^4T_1$ sublevels of 22 and 4.14 cm^{-1} as obtained from the experiments is indicated.

In all these cases the static limit of the Jahn-Teller interaction is realized. For example, in GaP:Mn^{2+} (Refs. 12 and 13) two peaks that are separated by 10 cm^{-1} have been resolved. Similar twofold splittings are reported for ZnS:Mn^{2+} (10 cm^{-1}) (Refs. 14 and 15) and ZnSe:Mn^{2+} (11.5 cm^{-1}).[15] Recently similar spectroscopic structures were also found for $Fe^{3+}(3d^5)$ in ZnS (4.7 cm^{-1}) (Ref. 16) and GaAs:Fe^{3+}.[17]

The relatively strong and structured phonon replica and the fine structure of the ZP line give evidence for a Jahn-Teller effect in the 0.5-eV luminescent center. For the present case the $^4T_1$ state is split at least into three states, where the upper excited states are separated by 4.14 and 22 cm^{-1} from the lowest $^4T_1$ level, respectively (Fig. 5). Most probably the excited state is split into four levels as discussed in Sec. III (this is indicated by the additional broken line in Fig. 5). Hence the Jahn-Teller distortion does not reach the static limit.

But relaxation effects of the defect alone cannot explain why the ZP lines are unusually weak compared to the sideband spectrum. In total we find the contribution of the ZP transitions to be less than $\frac{1}{500}$ of the total luminescence. If the intensity relation between the ZP lines and the GM$_2$ replica would only be determined by a high Huang-Rhys factor the transitions into higher phonon states like 2$\times$GM$_2$, 3$\times$GM$_2$, ... should even be more pronounced. As can be seen in Fig. 1 this is not the case: the 2$\times$GM$_2$ replica is smaller than GM$_2$. Weak or missing ZP transitions when phonon replicas are present are known for so-called "forced electric-dipole transitions" as discussed by Loudon.[18] When the ZP transition is

forbidden the vibrational sidebands can gain oscillator strength by an admixture of appropriate states induced by electron-phonon coupling. Obviously this effect governs the optical transitions in the 0.5-eV center. In the model discussed above, the ZP transitions between pure $^4T_1(^4G)$ and $^6A_1$ states are not electric-dipole allowed because of the selection rule $\Delta S = 0$. Only mixing between $^4T_1(^4G)$ and $^6A_1$ states induced by the spin-orbit coupling makes the optical ZP transitions weakly allowed. Therefore in the vibronic sideband the oscillator strength reacts sensitively on admixtures. Most probably the symmetry properties of the vibronic gap modes which determine the kind of electronic admixture are responsible that GM_2 appears much stronger than GM_1 and GM_3 (Fig. 1, left inset).

A long decay time τ of the luminescence (milliseconds) is also characteristic of spin-flip transitions, e.g., $\tau = 1.5$ ms was found for GaP:Mn^{2+}.[12] The corresponding transitions of $Fe^{3+}(3d^5)$ also show long-time constants. Recently for the systems ZnS:Fe^{3+} and GaAs:Fe^{3+} a time constant for the transient PL signal of 4.3 (Ref. 16) and 1.9 ms,[17] respectively, was obtained.

The decay time of the 0.5-eV luminescence band is 1.1 ms and thus two orders of magnitude larger than the decay time that was found for the Fe^{2+} transition (10 μs). This fact clearly rules out the previous assignment of the underlying center to a Fe^{2+}-related complex. Moreover, the long decay time clearly supports the interpretation as an Fe^{3+} internal spin-flip transition. In accordance with this result the 0.5-eV emission is either observed only weakly or is not detectable in n-type material.

We will now turn to the excitation mechanism of both the 0.5- (Fe^{3+}) and the 0.35-eV (Fe^{2+}) luminescence. As shown in Sec. III B there is an efficient energy transfer from the bound CT states of [$Fe^{2+}(^5T_2)$, h_b] to the 0.5-eV center. This fact gives strong evidence that all the optical processes reported here occur at one center, and hence that Fe^{3+} is the responsible center for the 0.5-eV luminescence band. An energy transfer of similar efficiency from bound CT states of Fe^{2+} to a locally separated Fe-related complex seems to be rather unlikely, because free carriers are not involved.

Klein *et al.*[9] have analyzed by time-resolved PL measurements how the characteristic Fe^{2+} luminescence at 0.35 eV can be excited by the capture of free carriers. The PLE data [Fig. 4(c)] reflect this, too, and show an additional excitation mechanism. We observe (i) the well-known photoexcitation band due to the generation of free holes [$Fe^{3+} \rightarrow Fe^{2+}(^5T_2) + h$],[6] (ii) positive peaks of the series $A_1, \ldots, A_3$ and $B_1, \ldots, B_3$ due to the excitation of Fe^{3+} into the CT states of Fe^{2+}: ($Fe^{3+} \rightarrow$ [$Fe^{2+}(^5T_2)$, h_b]), where the hole remains bound in the EMT states (h_b). The latter process requires that the hole remains bound to the Fe^{2+} while the optical transition (0.35 eV) occurs. But as the hole is attracted by the negatively charged Fe^{2+} ion a recombination process of the type [Fe^{2+}, h_b] $\rightarrow$ (Fe^{3+})* is also possible. This recombination leaves the Fe^{3+} ion in an excited state (Fe^{3+})* which acts as a source for the 0.5-eV band.

In principle there are two states where the recombination can occur, the Fe^{2+} excited state $^5T_2$ and the ground

state ^5E. While in the latter case the 0.5-eV emission simply follows after the 0.35-eV emission, the Fe^{3+} luminescence directly competes with the 0.35-eV optical transition in the first case. For this fact we find experimental evidence from PLE [Figs. 4(b) and 4(c)] as well. On the one hand the resonances (A_1+GM1*) and (A_1+RM1*) appear as dips in the 0.35-eV PLE spectrum; on the other hand the same resonances show up as peaks in the 0.5-eV PLE spectrum. Evidently, the Fe^{2+} luminescence is not efficiently excited via bound CT states. In Fig. 4(c) only at around 9100 to 9300 cm^{-1} when photoionization is relatively weak a notable positive contribution is found. At around 9500 cm^{-1} when photoionization becomes more important the CT resonances consume excitation power which mainly will serve for the Fe^{3+} luminescence. Thus we find dips in the PLE of Fe^{2+} but peaks in the PLE of Fe^{3+}. Because the hole is already localized in the CT states the recombination probability is higher than for the Fe^{2+} states, which have to capture a free hole.

The present data are summarized in the scheme of Fig. 6, where the excitation mechanism of the Fe^{3+} emission is depicted in the right part. The manifold of $3d^5$ states of Fe^{3+} is depicted. On the left-hand side the CT state is represented by the $3d^6$ states of Fe^{2+} where we omit the EMT states of the bound hole.

The relaxation within the Fe^{3+} ion to populate the $^4T_1$ first excited state can either be radiative or nonradiative. One possibility is that the Fe^{3+} ion is left in an excited state of, e.g., ^4P or ^4F after the hole capture (compare Figs. 5 and 6), and then relaxes radiatively to the $^4T_1(^4G)$ state. As shown in Sec. III the feature X at around 4120 cm^{-1} (Fig. 2) does not fit to any phonon coupling. Therefore this structure could be due to a ra-
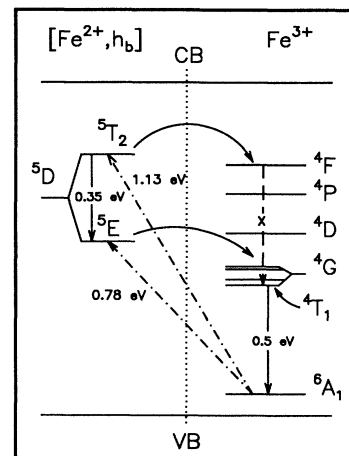

FIG. 6. Energy transfer from Fe^{2+} to Fe^{3+}. In the PLE experiment the CT states [$Fe^{2+}(5T_2, {}^5E)$, h_b] are first excited resonantly from Fe^{3+} (broken lines). Then the hole h_b, which is bound by Coulomb attraction to Fe^{2+}, recombines with Fe^{2+} in the $^5T_2$ or in the ^5E state. The Fe^{3+} ion is left in an excited state (Fe^{3+})*. Electrical dipole-allowed transitions X (4120 cm^{-1}) lead to the lowest excited state $^4T_1(^4G)$ prior to the spin-flip transition $^4T_1 \rightarrow {}^6A_1$ (4300 cm^{-1}). In this level scheme spin-orbit splitting is omitted.

diative transition within the Fe^{3+} ion from a highly excited state $(Fe^{3+})^*$, e.g., ^4F or ^4P to the $^4T_1(^4G)$ first excited state. The large half-widths can be explained by lifetime broadening of the excited state ^4F.

Finally, we compare the vibronic properties found for Fe^{3+} with those of Fe^{2+}. For Fe^{3+} we find vibrational gap modes GM_1 through GM_3 and vibrational resonant modes RM_1 and RM_2. The corresponding phonon energies (Table I) are clearly distinct from those of the vibrational modes ($GM1$: 295 cm^{-1} and $LM1$: 350 cm^{-1}) found for Fe^{2+}.[3] A line quintet at 6200 cm^{-1} observed in calorimetric absorption spectroscopy,[19] but not shown here, was recently ascribed to an exciton deeply bound at Fe^{3+}.[19,20] From the data presented here this assignment is rather unlikely because the vibronic sideband of the quintet clearly shows the properties of Fe^{2+} (Refs. 3 and 4) but not of Fe^{3+}. Therefore the assignment of the excited state of the line quintet to $[Fe^{2+}(^5E), h_b]$ as given in Ref. 4 is fully consistent with our results.

V. CONCLUSION

By PL (excitation) spectroscopy we study the 0.5-eV luminescence band in InP:Fe. We assign these emissions to $^4T_1 \rightarrow {}^6A_1$ (spin-flip) transitions of $Fe^{3+}(3d^5)$. Our findings clearly discard earlier assignments to $^5D(3d^6)$ transitions of Fe^{2+}-related complexes or to a charge-transfer reaction $(Fe^{3+} \rightarrow [Fe^{2+}(^5T_2), h_b])$. A fine structure is found in the zero-phonon lines and hints to a dynamic Jahn-Teller effect inherent in the $^4T_1$ excited states. The spin-flip transitions show a long decay time of 1.1 ms, which is more than two orders of magnitude longer than the time constant of the $3d^6$ transitions of Fe^{2+} (10 μs). We observe efficient energy transfer from the charge-transfer states $[Fe^{2+}(^5T_2), h_b]$ and $[Fe^{2+}(^5E), h_b]$ to the luminescent state $^4T_1$ of Fe^{3+}. The vibrational modes of Fe^{3+} are clearly distinct from the vibrational modes of Fe^{2+}. Therefore we reject the interpretation of the quintet structure at 6200 cm^{-1} in SI-InP:Fe as an exciton deeply bound at Fe^{3+}.

ACKNOWLEDGMENTS

[1]G. W. Isler, S. J. Pearton, and B. J. Sealy, *Properties of Indium Phosphide* (The Institution of Electrical Engineers, London, 1991), p. 25.

[2]W. H. Koschel, U. Kaufmann, and S. G. Bishop, Solid State Commun. **21**, 1069 (1977).

[3]K. Pressel, K. Thonke, A. Dörnen, and G. Pensl, Phys. Rev. B **43**, 2239 (1991).

[4]K. Thonke and K. Pressel, Phys. Rev. B **44**, 13 418 (1991).

[5]P. R. Tapster, M. S. Skolnick, R. G. Humphreys, P. J. Dean, B. Cockayne, and W. R. MacEwan, J. Phys. C **14**, 5069 (1981).

[6]P. Leyral, G. Bremond, A. Nouailhat, and G. Guillot, J. Lumin. **24/25**, 245 (1981).

[7]B. Deveaud, G. Guillot, P. Leyral, C. Benjeddou, A. Nouailhat, and B. Lambert, in *Proceedings of the 4th Conference on Semi-insulating III-V Materials, Kah-nee'ta, 1983*, edited by D. C. Lock and J. S. Blakemore (Shiva, Nantwich, 1984), p. 493.

[8]*Numerical Data and Functional Relationships in Science and Technology*, Landolt-Börnstein, New Series, Group X, Vol. 17, Pt. a (Springer-Verlag, Berlin, 1982), pp. 281ff.

[9]P. B. Klein, J. E. Furneaux, and R. L. Henry, Phys. Rev. B **29**, 1947 (1984).

[10]T. Kushida, Y. Tanaka, and Y. Oka, Solid State Commun. **14**, 617 (1974).

[11]P. Koidl, Phys. Status Solidi B **74**, 477 (1976).

[12]A. T. Vink and G. G. P. Van Gorkom, J. Lumin. **5**, 379 (1972).

[13]G. Hofmann, F. G. Anderson, and J. Weber, Phys. Rev. B **43**, 9711 (1991).

[14]M. Zigone, R. Beserman, and B. Lambert, J. Lumin. **9**, 45 (1974).

[15]R. Parrot, C. Naud, C. Porte, D. Fournier, A. C. Coccara, and J. C. Rivoal, Phys. Rev. B **17**, 1057 (1978).

[16]A. Hoffmann, R. Heitz, and I. Broser, Phys. Rev. B **41**, 5806 (1990).

[17]K. Pressel, G. Bohnert, G. Rückert, A. Dörnen, and K. Thonke, J. Appl. Phys. **71**, 5703 (1992).

[18]R. Loudon, Proc. Phys. Soc. **84**, 384 (1964).

[19]A. Juhl, A. Hoffmann, D. Bimberg, and H. J. Schulz, Appl. Phys. Lett. **50**, 1292 (1987).

[20]A. Görger and J-M. Spaeth, Semicond. Sci. Technol. **6**, 800 (1991).